Effects of various cutting treatments and topographic factors on microclimatic conditions in Dinaric fir-beech forests

Janez Kermavnar*[1], Mitja Ferlan[1], Aleksander Marinšek[1,3], Klemen Eler[2,1], Andrej Kobler[4], Lado Kutnar[1]

[1]Slovenian Forestry Institute, Department of Forest Ecology, Večna pot 2, 1000 Ljubljana, Slovenia

[2]University of Ljubljana, Biotechnical faculty, Department of Agronomy, Jamnikarjeva ulica 101, 1000 Ljubljana, Slovenia

[3]Higher Vocational College for Forestry and Hunting, Ljubljanska cesta 2, 6230 Postojna, Slovenia

[4]Slovenian Forestry Institute, Department of Forest and Landscape Planning and Monitoring, Večna pot 2, 1000 Ljubljana, Slovenia

*Corresponding author: Tel.: +38612007831, e-mail: janez.kermavnar@gozdis.si

Published in Agricultural and Forest Meteorology, Volume 295, 15 December 2020, 108186

https://doi.org/10.1016/j.agrformet.2020.108186

Abstract

Forest microclimate is strongly affected by local topography and management activities, as these directly alter overstory structure. In the present work we analysed the dependence of observed patterns of spatio-temporal microclimatic variations on topographic, canopy- and management-related factors. A forestry experiment was conducted in managed fir-beech forests in the Dinaric Mountains (Slovenia), which are characterized by rugged karstic terrain with numerous sinkholes. In 2012, cutting treatments representing a range in the intensity of overstory removal were performed: uncut controls (CON), 50% cut of stand growing stock (intermediate management intensity – IMI) and 100% cut (high management intensity – HMI) creating 0.4 ha canopy gaps. Fine-scale variation in aspect and slope and its effects on microclimate was assessed by comparing central, south-facing and north-facing within-sinkhole positions. We measured microclimatic variables (air temperature – T, relative humidity – RH) 0.5 m above the ground over three consecutive post-treatment growing seasons. Microclimatic variables showed an increase (T and vapour pressure deficit – VPD) or decrease (RH) with management intensity. Daily T_{max} and VPD_{max} in HMI treatment were up to 5.9 °C (on average 3.5 °C) and up to 1.4 kPa (on average 0.6 kPa) higher than those in CON treatment, respectively, whereas daily RH_{min} was up to 22.7 (on average 13.0) percentage points lower. Regarding intra-seasonal patterns, microclimatic differences between treatments were largest during the summer. South-facing plots in the HMI treatment overall exhibited the most extreme conditions, i.e. the highest T_{max} and lowest RH_{min}. Differences in microclimate between treatments were strongly modulated by canopy cover. The results also suggest that overstory removal increases topography-mediated variation in microclimate, as evidenced by significant differences in T, RH and VPD along the fine-scale topographic gradient within the created canopy gaps.

Key words: tree cutting; air temperature; relative humidity; vapour pressure deficit; karst topography; canopy cover

1. Introduction

Trees and forest stands are known for their marked impact on local (micro)climate (Aussenac, 2000; Renaud et al., 2010). Forest ecosystems function as a thermal insulator, meaning that the daytime air temperature is lower, the daily temperature range is smaller and it is warmer during the night compared to forest edges and canopy gaps without tree canopies (Chen et al., 1993; Kovács et al., 2017; De Frenne et al., 2019). Owing to sheltering from direct insolation and increasing evaporative cooling (Thom et al., 2020), forests are often referred to as specific abiotic environments where microclimatic conditions can significantly deviate from the regional macroclimate (Frey et al., 2016; Macek et al., 2019). Decoupling between microclimate and macroclimate has important implications for the forest biota living in these environments (Zellweger et al., 2019). Such buffering effects are directly influenced by silvicultural measures, which primarily alter the structure of forest stands (Zheng et al., 2000; Aussenac, 2000; Ehbrecht et al., 2019). The formation of canopy gaps induces higher levels of direct short-wave solar radiation reaching the forest floor and greater losses of outgoing long-wave radiation from soils. The modulation of the light regime is expected to be the main process through which canopy openings influence forest microclimate (Thom et al., 2020). For example, Abd Latif and Blackburn (2010) demonstrated that the air temperature in gaps was influenced directly by the amount and duration of solar radiation received.

Apart from the direct effects of forest management on microclimate, other environmental factors (e.g. local topography, soil characteristics) have been proven to be very important for differences in microclimate at smaller spatial scales, particularly in areas with heterogeneous topographical setups (Grimmond et al., 2000; Frey et al., 2016; Greiser et al., 2018), such as karst landscape. Topographically driven spatial variability of microclimate and soil properties are expected to be the most clearly expressed in mountainous landforms (Cantlon, 1953). Even so, these ecological phenomena also apply to lowland areas (e.g. Sewerniak et al., 2017; Sewerniak and Puchałka, 2020). As such, the effects of tree cutting might interact with these factors, inducing more complicated patterns in microclimatic variables. For instance, differences in aspect position and slope inclination induce changes in incident radiation and soil moisture (Sewerniak et al., 2017), resulting in large variability in temperature and relative humidity over micro- and meso-scales (Ashcroft and Gollan, 2013; Macek et al., 2019). The influence of local terrain features on microclimate dynamics is even expected to be largely independent from the effects brought about by local canopy characteristics (Zellweger et al., 2019). However, it remains unclear whether topography-induced spatial variability of forest microclimate increases after management disturbance. Fine-scale variation in microclimate and associated soil properties (Kobal et al., 2015; Sewerniak et al., 2017; Jasińska et al., 2020) may have important implications for habitat and species diversity and composition within intact forests and canopy gaps (Suggitt et al., 2011; Jucker et al., 2018; Macek et al., 2019). Microclimatic conditions in forests with diverse topography can decouple from macroclimate to such degree that specific relief positions (e.g. topographic concavity caused by depressions of karst surface) may even serve as potential microrefugia for some species under the climate change (Lenoir et al., 2017; Kiss et al., 2020; Bátori et al., 2020).

The need for knowledge on the effects of forest management on microclimate has long been recognised (Keenan and Kimmins, 1993). Microclimate has a significant impact on tree species regeneration and plant growth and is a major driver of ecosystem processes such as decomposition, soil respiration and nutrient dynamics (Ma et al., 2010). Previous studies have either studied the main structural determinants of mature forest stands on microclimate, mainly on temperature (e.g. Ehbrecht et al., 2019), or compared the below-canopy environment to that of the adjacent open area (e.g. von Arx et al., 2012). Additionally, extensive work has been dedicated to the quantification of how different forest management practices affect key abiotic variables (e.g. Heithecker and Halpern, 2006; Heithecker and Halpern, 2007; Kovács et al., 2017; Thom et al., 2020). Nevertheless, disturbance impacts on microclimate remain poorly quantified, despite the importance of microclimatic conditions for future forest development. Furthermore, previous studies have rarely been based on controlled manipulation experiments (Thom et al., 2020). Such studies usually showed the most profound differences in microclimate between intact stands (control) and conditions found in more open areas such as clear-cuts. When studying forest microclimate, it is important not only to describe the average conditions of cutting treatments but also the magnitude or sources of variation within them (Heithecker and Halpern, 2006; Abd Latif and Blackburn, 2010). Evaluating the influence of management practices on microclimatic variation and monitoring microclimate over the long term are essential for improving our understanding of forest resources and effectiveness in managing them (Zheng et al., 2000).

In this study we examined patterns of microclimatic variation among silvicultural treatments that represent a gradient in cutting intensity in mixed forests in the Dinaric Mountains. To some degree, changes in microclimate due to forest management may be predictable. Although considerable information has been published on the effects of different levels of overstory removal upon microclimate, its topography-modulated spatial variability remains poorly understood in general. Because of the accentuated karst topography of the Dinaric region, we expect that variation in local topographic factors (aspect and slope) will strongly interact with silvicultural measures to influence microclimatic conditions in the studied forest type.

Our objectives were to (1) quantify cutting treatment effects on microclimate, (2) examine fine-scale spatial variation in microclimate associated with local topographic factors (i.e. slope aspect and inclination) and forest structure (i.e. canopy cover), and (3) assess the potential interplay between forest management and local topography. Their combined influence on microclimatic conditions has received little notice so far. Effects of topographic factors upon forest microclimate seems to be universal, most often evidenced by the comparisons between south- and north-facing slopes in both concave and convex configurations. We aim to confirm certain generalities that can be drawn from earlier studies, conducted in widely different climatic regions, topographical setups and forest types. This will help to assess the impacts of relatively small-scale landforms (karst sinkholes in our case) on microclimate, further solidifying their prominent ecological role in shaping forest structure and vegetation composition (Kobal et al., 2015), as well as concerning the post-disturbance successional trajectories.

2. Materials and methods

2.1. Study area

This study was conducted at three distinct study sites (Kočevski Rog, Snežnik and Trnovo) in Slovenia, all of which are covered by Dinaric fir-beech forests. The study area at each site was ca. 70 ha in size. For more details about our study area, see Kutnar et al. (2015). Despite being located tens of kilometres apart, regional climatic conditions, characteristics of stand structure (tree species composition, stand age, understory development) and general topographic appearance (karst landscape) were similar across the study sites. In general, the climate is moderate continental, i.e. warm, dry summers and cold, wet winters. The mean annual temperature is 8–9 °C and mean annual precipitation is 1700–2000 mm (Kutnar et al., 2015). The topography is characterized by diverse karst terrain with numerous sinkholes (bowl-shaped depressions, also known as karst dolines; Aguilon et al., 2020), ridges and slopes. The diversity of the karst terrain results in small-scale heterogeneity in edaphic conditions. The most frequent soil types are Eutric Cambisols (calcareous brown forest soils), Leptosols (rendzinas) and Luvisols (IUSS Working Group WRB, 2015) derived from limestone and dolomite parent materials. The vegetation consists of uneven-aged Dinaric fir-beech forests affiliated to the *Omphalodo–Fagetum* s. lat. association, with the stand growing stock ranging between 300 and 400 $m^3 \cdot ha^{-1}$ (Kutnar et al., 2015). Before cutting, all of the stand overstories were dominated by European beech (*Fagus sylvatica* L.), silver fir (*Abies alba* Mill.) or Norway spruce (*Picea abies* (L.) Karst.) and were most often a mixture of these late-successional tree species.

Pre-treatment forests were characterized by homogeneous mature stands with well-developed vertical stratification and dense canopy cover (~ 95%) and lacked evidence of recent management or natural disturbances. Local regeneration patches of irregular size and shape were thus limited. The investigated forest stands have a heterogeneous structure with trees of different diameters and heights. Continuous-cover and close-to-nature silvicultural approaches that support structural heterogeneity have been traditionally used. Single-tree and group-selection cuttings are most frequent measures to initialize tree regeneration in the studied forests (Kutnar et al., 2015). Unfragmented forests in the Dinaric Mountains represent one of the few large forested landscapes in Europe with continuous canopy cover, where stand-replacing disturbances happen only infrequently (Nagel et al., 2017).

2.2. Experimental design and sampling procedures

At each of the three study sites, nine karst sinkholes were randomly selected, amounting to 27 sinkholes in total for the entire study area. The basic geomorphological parameters of the sinkholes (i.e. elevation, size, shape) were comparable between treatment types (see Table S1 in the Supplementary material). Average distances between the centres of the selected sinkholes were 562.9 m (Kočevski Rog), 524.4 m (Trnovo) and 399.2 (Snežnik), respectively, with an overall mean of 495.5 m.

In each sinkhole, a circular treatment area of 0.4 ha (r = 35.7 m) with the centre in the bottom of the sinkhole was established. The sinkholes were randomly assigned to three different cutting intensities (forest management treatments): (a) control with no cutting of the overstory trees (control – CON), (b) 50% cutting of the initial stand growing stock with residual trees being evenly spatially distributed across the treatment area (intermediate management intensity – IMI) and (c) 100% cutting of the growing stock with no mature trees remaining (high management intensity – HMI). In silvicultural terms, IMI is a form of uniform partial cutting that is comparable to intensive thinning or dispersed tree retention. In the HMI treatment 0.4 ha circular canopy gaps were formed within the surrounding closed canopy stands. The canopy gaps created are substantially smaller than is typical in European temperate deciduous forest (3–10 ha) (Kovács et al., 2018) but are in conformity with Slovenian legislation (Forest Act, 1993), which generally prohibits forest "clear-cuts" exceeding 0.5 ha. Within each study site, the pre-treatment conditions of the sinkholes selected for the different treatment levels were comparable. Cutting of trees and hauling of logs was completed in 2012.

Our sampling procedure was specifically designed to assess environmental variation due to both management-induced canopy effects and topographic (slope exposition) variability. Within each sinkhole, three measuring plots were established: in the sinkhole centre/bottom (C) and on its south-facing (S) and north-facing (N) slopes (Fig. 1). Due to bowl-shaped topographic concavity, northern within-sinkhole positions/plots have south-facing exposure and southern within-sinkhole positions/plots have north-facing exposure. The south-facing and north-facing plots were 12 m from the bottom/centre of the sinkhole (Fig. 1). In total, 81 plots (27 sinkholes × three within-sinkhole positions) were established, and data on meteorological variables, overstory structure and topographic factors were collected.

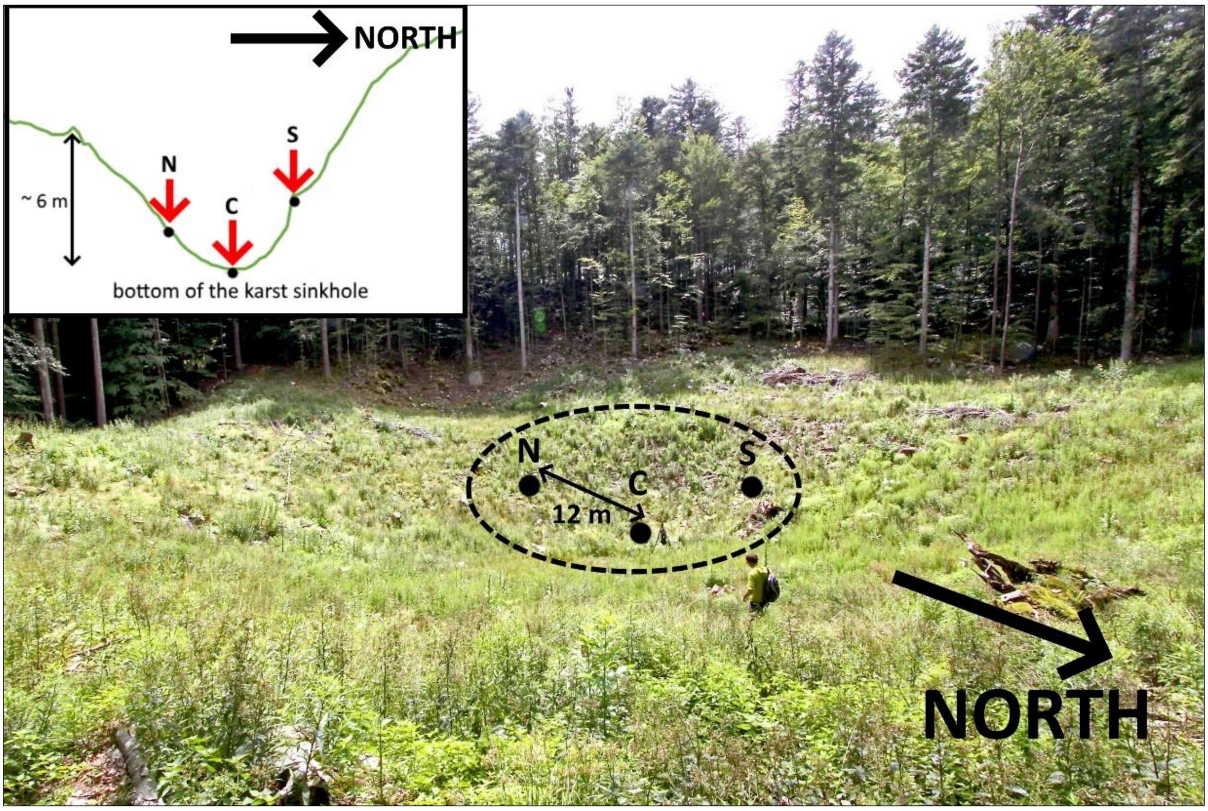

Figure 1: An example of the HMI treatment with the positions of three plots within a karst sinkhole, where data on microclimatic and other environmental conditions were measured. One plot was established in the centre (i.e. bottom of the sinkhole, C), one in the south-facing (S) and one in the north-facing (S) slope of the sinkhole, 12 m from the bottom/centre of the sinkhole. The dashed ellipse denotes the approx. edge of the sinkhole. The vertical profile of the sinkhole is shown in the upper left corner. Photo by Lado Kutnar, July 2014 (i.e. 2 years after cutting).

2.3. Data collection

Microclimatic measurements were carried out with a Voltcraft DL-120 TH (Conrad Electronic SE, Hirschau, Germany) data logger with an SHT11 integrated sensor (Sensirion Inc.) for air temperature (T, in °C) and relative humidity (RH, in %). Sensors (with typical accuracy of ± 0.4 °C and ± 3%, respectively) were installed 0.5 m above the ground surface and were inserted into radiation shields to protect the instruments against direct solar radiation. Data loggers were programmed to record T and RH every 30 minutes. Measurements were deployed over three consecutive growing seasons: immediately after cutting in 2012 and in the next two years. Sensors collected meteorological data in the period of canopy leaf-out, when canopy closure was fully developed, i.e. from May to October.

To evaluate potential differences in microclimate due to variation in topography, we collected the aspect (azimuth in ° from the north) and slope inclination (in °) at each plot.

Percent canopy closure was determined from aerial LiDAR scanning performed in 2013. First, the canopy height model (CHM) with 1 m horizontal resolution was calculated from the lidar point cloud. Three concentric circular areas with radii of 2 m, 4 m and 8 m, respectively, were defined. The centres of these areas were coincident with the sampling plot centres. Canopy cover in each circular area was then expressed as the percentage of the area covered by CHM vegetation higher than 5 m. Thus, we not only considered canopy cover in the plot but also in its variously sized neighbourhoods. Based on visual estimation, there were no evident changes in overstory canopy cover in the post-treatment period.

2.4. Data preparation and processing

Microclimate data series were first graphically and quantitatively inspected. Statistical outliers and data points indicating obvious errors caused by sensor failures (e.g. unrealistic data or large spikes in variables) were detected with the 'tsoutliers' function in the R package *forecast* (Hyndman et al. 2019; R Development Core Team, 2018) and then omitted from the analysis. The temperature data coherence for each plot was checked by comparison with daily data from the nearest meteorological station at each study site for each growing season (data retrieved from Slovenian Environment Agency archive, 2019); generally, the correlation coefficients were above 0.9 (data not shown).

For a few plots, some minor data on T and RH were missing due to technical failures of sensors or empty batteries. In the case of T, missing 30 min values were gap-filled using linear regressions between the plot and nearest meteorological station because the correlations were strong (Pearson's coefficients > 0.9). For RH, the correlation coefficients between our plots and the nearest meteorological stations were very low (usually below 0.1). Therefore, to gap-fill RH data, linear regressions between the missing RH data and complete T data from the nearest plot were used.

Based on T and RH gap-filled data, the vapour pressure deficit (VPD, in kPa) was calculated for each sensor (plot) at each time step (30 min) using the formula:

$$VPD = e_{sat} - e_{air}$$

where e_{sat} is the saturation vapour pressure and e_{air} is the air (actual) vapour pressure (Murray, 1967). A combination of high T and low RH produces high VPD values (Ashcroft and Gollan, 2013). VPD is an eco-physiologically meaningful climate variable and a good standalone indicator of the atmospheric factors influencing evapotranspiration (Jucker et al., 2018). A higher VPD implies increasing water stress of plants (Thom et al., 2020). Although temperature extremes have been more frequently studied, the critical role of VPD for plant growth and survival is increasingly recognized (Davis et al., 2019).

To quantify the effects of topographic factors on microclimate, we derived an index called "AspSlo", which combines slope aspect and slope inclination and expresses the aspect-related radiative exposure (Fleming and Baldwin, 2008). It was calculated with the following formula:

$$AspSlo = ((cos[ABS(225° - \Theta)] \times sin(\alpha))$$

where Θ is aspect (°) and α is inclination (°); both parameters need to be transformed to radians before calculation. In the formula above, 225° expresses the southwestness (Heithecker and Halpern, 2006); slopes in the northern hemisphere with south-western orientations are expected to receive the highest amount of solar radiation. However, this also depends on slope steepness – steeper slopes are more exposed to radiation than flat areas. In theory, the AspSlo index ranges from -1 (aspect = 45°, slope = 90°) to 1 (aspect = 225°, slope = 90°).

2.5. Calculation of aggregated microclimatic values

For each microclimatic variable (T, RH and VPD), the data sets contained almost two million individual data points (30 min records), when the data from the three study sites and three growing seasons were pooled.

The 30 min observations were aggregated into different daily values. We focused on four main variables: daily maximum temperature (T_{max}), diurnal temperature range (DTR) as the difference between T_{max} and daily minimum temperature (T_{min}), minimum relative humidity (RH_{min}) and maximum vapour pressure deficit (VPD_{max}). Mean daily values (T_{avg}, RH_{avg}, VPD_{avg}) were calculated as well. For each treatment type, daily values for each sensor (plot) were averaged across each growing season and also over three growing seasons to obtain the overall mean plot-level value.

In addition, we calculated microclimatic differences (marked with Δ) between three cutting treatments: CON vs. HMI, CON vs. IMI and IMI vs. HMI. Microclimatic differences between treated and untreated stands indicate the disturbance-induced change in the buffering capacity of intact forests with regard to T, RH and VPD. Control (CON) values were subtracted from the treatment values. For the IMI vs. HMI comparison, IMI values were subtracted from the HMI values. First, we averaged the values for each treatment, within-sinkhole position and day and then subtracted the control values, producing a daily difference. Then, the daily differences were averaged across the growing season. These were calculated for daily maximum temperature (ΔT_{max}), diurnal temperature range (ΔDTR), daily minimum humidity (ΔRH_{min}) and daily maximum VPD (ΔVPD_{max}). A separate analysis was done for the entire growing season (May–October, 184 days), the summer period (June, July, August; 92 days), which represents the most stressful portion of the growing season (e.g. summer drought, high temperature amplitudes and extremes; von Arx et al., 2013; Thom et al., 2020), and the transition period (May, September, October; 92 days).

Microclimatic variables were analysed in terms of their overall characteristics and patterns on different temporal scales. Intra-seasonal patterns of daily differences for the selected microclimatic variables were compared graphically. Second-order polynomial regression curves were fitted for each comparison. Similarly, diurnal patterns of T and RH were inspected with graphical visualisation, using 30 min data averaged across study sites, growing seasons and within-sinkhole positions.

2.6. Statistical analyses

To test how management intensity, within-sinkhole position and their interaction affect different microclimate variables over time, we constructed linear mixed-effects models. For modelling, the dependent variable means of each growing season were used (n = 243). Treatment (CON, IMI, HMI), position within the sinkhole (C, S, N) and growing season (2012, 2013, 2014) were regarded as fixed factors, while study site and sinkhole (nested within site) were specified as random factors. We used the Shapiro-Wilk test and graphical examination (histograms) to check whether each response variable significantly deviated from normal distribution. If so, appropriate data transformation was used (Faraway, 2006). To detect possible multicollinearity among the explanatory variables, we calculated variance inflation factors (Zuur et al., 2009). The models' goodness-of-fit values were measured by a likelihood-ratio test-based coefficient of determination (R^2_{LR}; Bartoń, 2019). For post-hoc tests, the Tukey procedure at alpha = 0.05 significance level was used.

We used simple linear regression to examine the relationship between overstory structure (canopy cover) and overall mean plot-level values of T_{max} and RH_{min} (averaged across the entire measurement period). Analysis of covariance (ANCOVA) was used to test for the effect of canopy cover on T_{max} and RH_{min}, in which treatment and study site were defined as covariates. Regression analyses were also used to investigate the dependence of microclimatic variables on topographic factors (AspSlo index), and this effect was tested with an ANCOVA (site and treatment as covariates in the model). This was done with the mean T_{max} and RH_{min} values for each sensor (n = 81) averaged across the entire measurement period.

All statistical analyses and graphing were conducted in R version 3.5.2 (R Development Core Team, 2018) using the following packages: *nlme* (Pinheiro et al., 2019), *multcomp* (Hothorn et al., 2019), *lsmeans* (Lenth, 2016) and *MuMIn* (Bartoń, 2019).

3. Results

3.1. The effects of cutting and within-sinkhole position on microclimate

According to the linear mixed models, treatment intensity had a highly significant effect on all of the microclimatic variables considered (Table 1). Treatment most significantly affected DTR, T_{max}, VPD_{max} and RH_{min}, whereas it showed a less strong effect on T_{min}, T_{avg}, RH_{avg} and VPD_{avg}. Mean and maximum T and VPD were on average highest in the HMI treatment and lowest in the CON treatment (Fig. 2). In contrast, mean and minimum daily RH were lowest in the HMI treatment. Daily T_{max} and VPD_{max} in the HMI treatment were up to 5.9 °C (overall average: 3.5 °C) and 1.4 kPa (0.6 kPa) higher than in the CON treatment, respectively, whereas daily RH_{min} was up to 22.7 (13.0) percentage points lower (Fig. 2). DTR was on average 4.2 °C higher in the HMI compared to the CON treatment. When comparing different treatments, the largest differences were between CON and HMI. Overall, for the analysed microclimatic variables, differences between IMI and HMI tended to be smaller than differences between IMI and CON (Fig. 2). Differences between treatments were higher for maximum and minimum variables compared to daily mean values.

The within-sinkhole position had a significant effect on some temperature variables (DTR, T_{max}, T_{min}) and vapour pressure deficit (VPD_{max}) (Table 1), but not in the CON treatment. The interaction between treatment and position showed a significant effect on DTR, T_{min} and T_{max} (Table 1). Along the cutting intensity gradient, differences between positions increased for all microclimatic variables (Fig. 2), with south-facing plots in the IMI and HMI treatments exhibiting the highest T_{max} and VPD_{max}. For example, the significance of the interaction term implies that there were larger temperature differences between the within-sinkhole positions in the IMI treatment, and particularly in the HMI treatment, compared to the CON treatment. North-facing plots in IMI and HMI tended to be colder and more humid compared to south-facing plots. Overall, the most extreme microclimatic conditions, i.e. high T and low RH resulting in high VPD, were in south-facing HMI plots (Fig. 2).

Table 1: The results of the linear mixed-effects models performed for the selected microclimatic variables: T – air temperature, RH – relative humidity, VPD – vapour pressure deficit, DTR = diurnal temperature range (T_{max} minus T_{min}). Interaction between position and growing season is not shown as it was not significant in any of the models. Captions: “avg” refers to mean, “max” to maximum and “min” to minimum.

Dependent variable	Model			Treatment		Position		G. season		Treat:Posit		Treat: g. season	
	Chi^2	*p*	R^2_{LR}	F	*p*	F	*p*	F	*p*	F	*p*	F	*p*
T_{avg}	355.06	***	0.799	32.94	***	2.47	ns	447.01	***	0.83	ns	-2.28	ns
T_{max}	287.45	***	0.845	261.97	***	11.31	***	72.74	***	3.32	*	4.92	***
T_{min}	321.82	***	0.734	32.29	***	6.30	**	291.94	***	3.69	**	3.28	*
DTR	233.45	***	0.836	376.34	***	15.93	***	10.56	***	4.19	**	5.35	***
RH_{avg}	277.25	***	0.742	48.37	***	0.76	ns	216.90	***	0.10	ns	2.08	ns
RH_{min}	222.91	***	0.777	141.84	***	2.77	ns	61.04	***	0.39	ns	3.20	*
VPD_{avg}	379.42	***	0.845	61.53	***	1.31	ns	440.60	***	0.49	ns	1.42	ns
VPD_{max}	335.87	***	0.846	217.30	***	7.32	**	149.24	**	1.70	ns	6.90	***

* $p < 0.05$, ** $p < 0.01$, *** $p < 0.001$, ns – not significant.

Treatment had a more prominent effect on the maxima and minima of the variables, while for the variable means (T_{avg}, RH_{avg}, VPD_{avg}), growing season proved to be more important (Table 1).

With respect to treatment effects, the largest differences in the investigated variables were detected between the CON and HMI treatments. These differences on average amounted to 3.5 °C (T_{max}), 4.2 °C (DTR), –13.0 percentage points (RH_{min}) and 0.6 kPa (VPD_{max}), respectively. The smallest differences were observed between the IMI and HMI treatments. Differences in microclimatic conditions were on average smaller between the IMI and HMI treatments than between CON and IMI treatments (Figs. 2b, 2d, 2f, 2h).

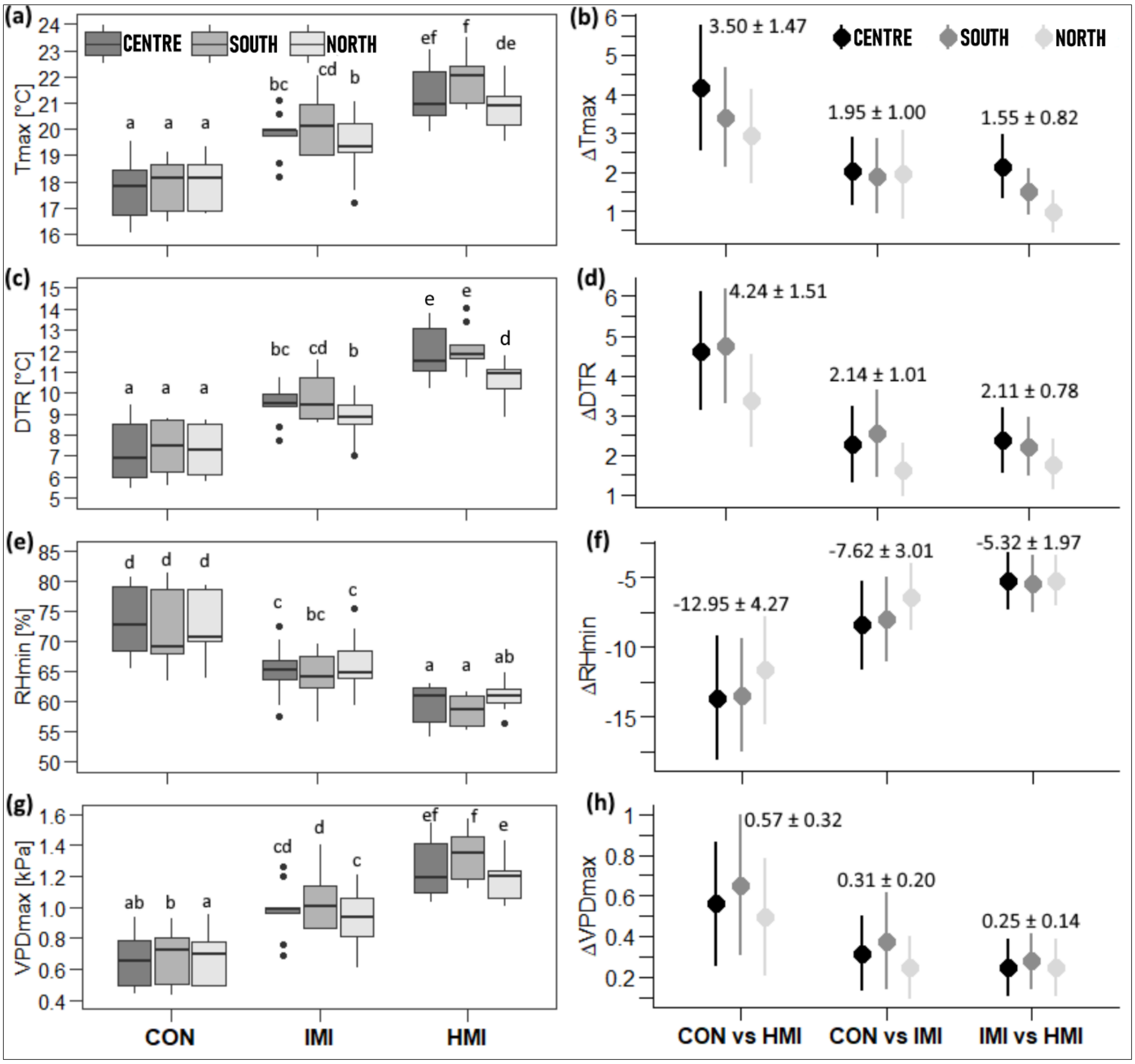

Figure 2: Plot-level values, averaged across three growing seasons, of four selected microclimatic variables: (a) daily maximum temperature (T_{max}), (c) diurnal temperature range (DTR = T_{max} minus T_{min}), (e) daily minimum relative humidity (RH_{min}) and (g) daily maximum vapour pressure deficit (VPD_{max}). Results are shown for each treatment (CON = control, IMI = 50% cut, HMI = 100% cut) and within-sinkhole position (centre – central plots, south – south-facing plots, north – north-facing plots). Letters designate significant differences between treaments and position. Panels b, d, f and h show differences (Δ, mean ± SD) in microclimatic variables between treatments.

3.2. Differences in microclimate between treatments: intra-seasonal variation

Differences between treatments in T_{max}, RH_{min} and VPD_{max} were largest during the summer months, especially in July and August (Fig. 3, Fig. S1 in the Supplementary material). These differences were in most cases smallest during the transition period (Fig. S1 in the Supplementary material). The strength of the cooling and humidifying effect of the canopy depended on the absolute value of T_{max}; the warmer the temperature, the stronger the canopy effect. For example, in the case of T_{max}, during a hot summer day with temperatures exceeding 30 °C, the difference between HMI and CON treatments reached 5 °C or even more. During colder days (e.g. temperatures between 10 and 15 °C), this difference was normally lower than 2 °C (data not shown). Similar patterns were observed for RH_{min} and VPD_{max} (Fig. 3).

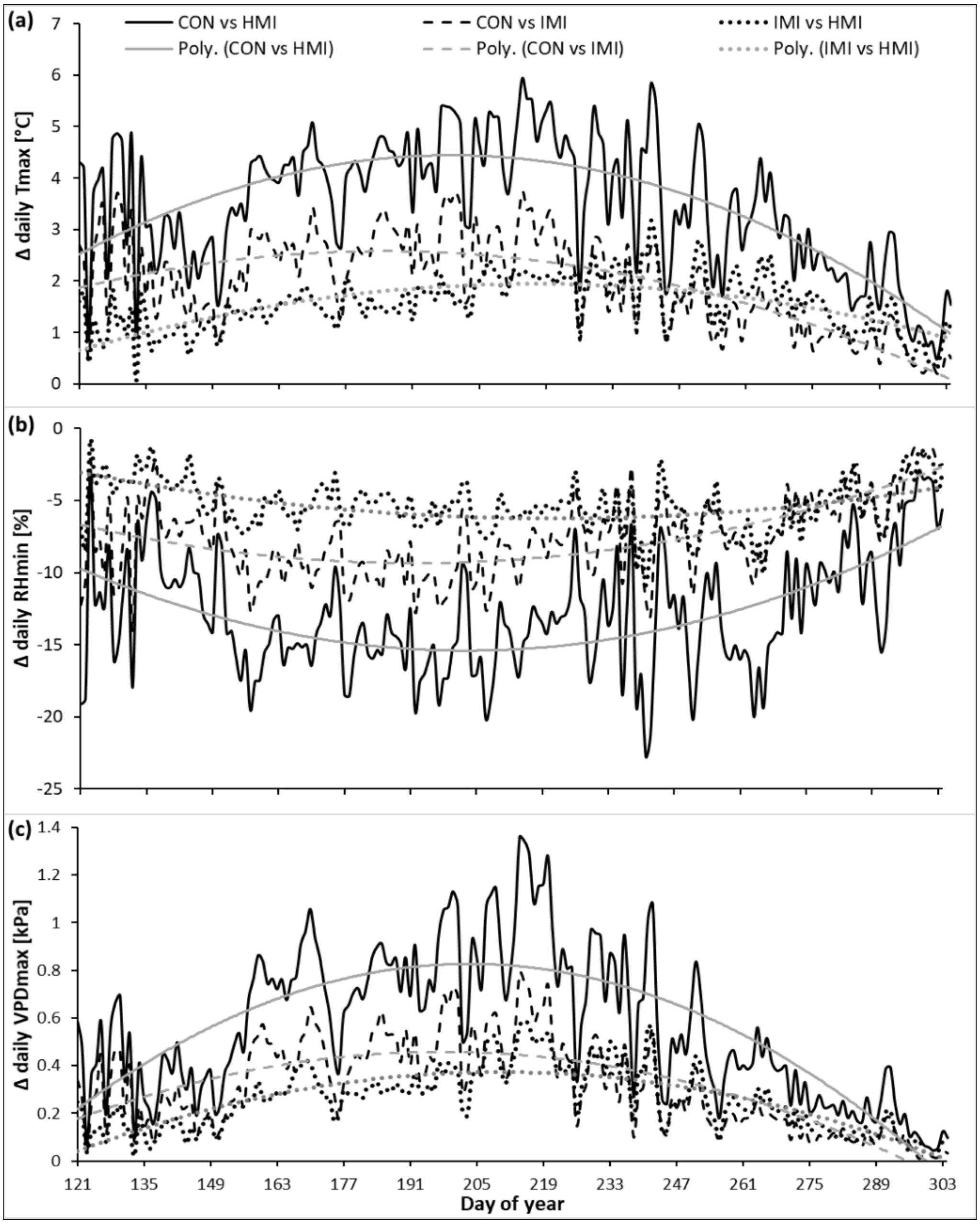

Figure 3: Mean temporal profile of differences between cutting treatments (CON = control, IMI = 50% cut, HMI = 100% cut) in (a) daily maximum temperature (T_{max}), (b) daily minimum relative humidity (RH_{min}) and (c) daily maximum (VPD_{max}) during the growing season (May 1 – Oct 31). The fitted curves (in grey) are second-order polynomial regression lines.

3.3. Diurnal course of air temperature and relative humidity

Intermediate management intensity and particularly HMI treatment experienced larger diurnal variation in T and RH values compared to the CON treatment (Fig. 4). Despite lower night-time temperatures in HMI treatment, the time of day when T_{min} was reached (at 04:30) did not differ between treatments. In contrast, air temperature in the HMI treatment reached its maximum ca. one hour before (at 12:30) peaking in the other two treatments (CON and IMI; at 13:30) (Fig. 4a). At peak time, T_{max} values (averaged across all days and across all growing seasons) reached 17.1 °C in the CON treatment, 18.4 °C in the IMI treatment and 19.9 °C in the HMI treatment (Fig. 4a).

Relative humidity, because of its coupling with T, showed a more or less inverse diurnal course compared to temperature (Fig. 4b). Its maximums were reached at 05:00 (IMI and HMI) and 06:00 (CON), respectively. Minimums of RH were reached almost at the same time as T peaked, i.e. at 12:30 (HMI) and 13:00 (CON and IMI). On average, at the time of the lowest daily RH (averaged across all days and across all growing seasons), values dropped to 76.7% in the CON treatment, 70.3% in the IMI treatment and 65.4% in the HMI treatment (Fig. 4b). Within-sinkhole position showed no effect on diurnal patterns of T and RH.

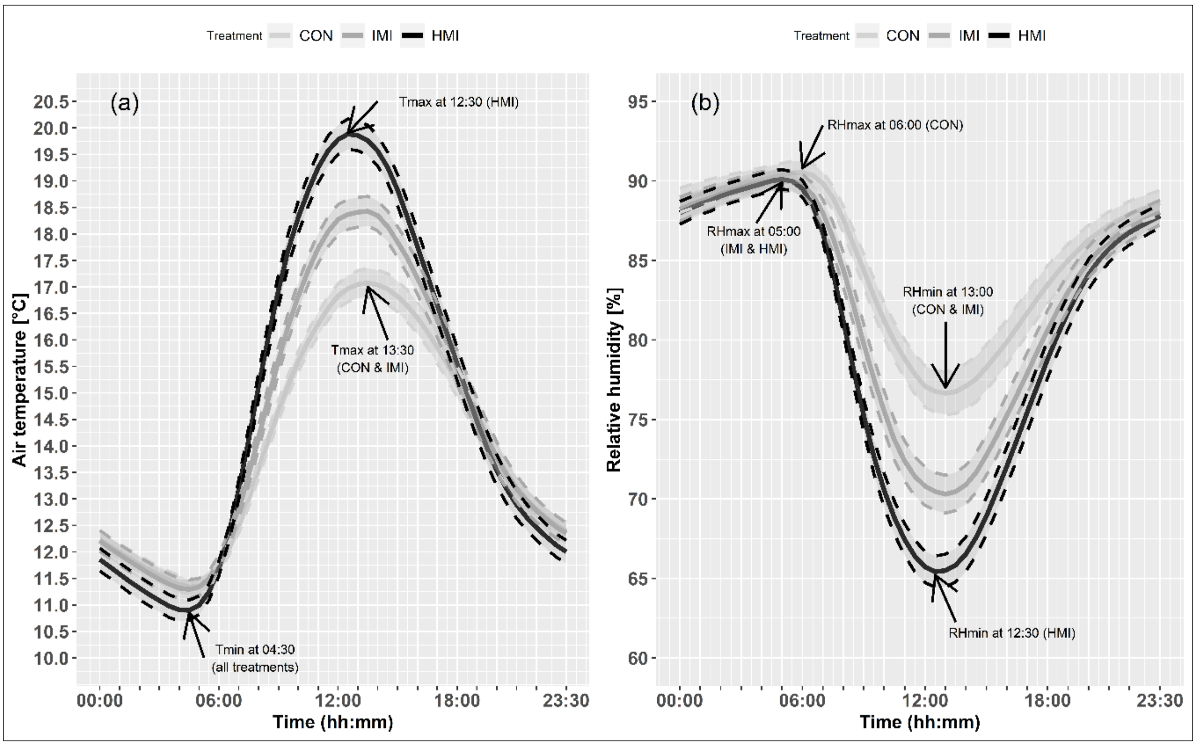

Figure 4: Diurnal course of (a) air temperature and (b) relative humidity for different cutting treatments (CON = control, IMI = 50% cut, HMI = 100% cut). Solid lines represent means averaged over the study sites, entire measurement period and within-sinkhole positions (i.e. central, south-facing and north-facing plots). Bands (dashed lines) represent 95% confidence intervals. Arrows indicate the time of day when peak values (maxima – max and minima – min) of microclimatic variables were reached for each treatment type.

3.4. *Relationship between overstory canopy cover and microclimatic variables*

Overstory vegetation characteristics (canopy cover) had a strong influence on T_{max} (ANCOVA: $n = 81$, $F_{1,75} = 342.3$, $p < 0.001$, $R^2 = 0.59$) and RH_{min} (ANCOVA: $n = 81$, $F_{1,75} = 262.5$, $p < 0.001$, $R^2 = 0.53$). Plots, which were subjected to different cutting treatments, exhibited wide variation in the degree of canopy closure (Fig. 5). There was a significant linear relation between canopy cover and daily T_{max}. Plots with higher overstory canopy cover (i.e. vegetation higher than 5 m) showed lower maximum temperatures and vice-versa. In contrast, we found a statistically significant positive linear relation between canopy cover and daily RH_{min}. Plots with higher canopy cover experienced higher humidity values and vice-versa (Fig. 5). Canopy cover also significantly affected other microclimatic parameters, i.e. T_{avg}, T_{min}, DTR, RH_{avg} and VPD_{avg} (ANCOVA results not shown).

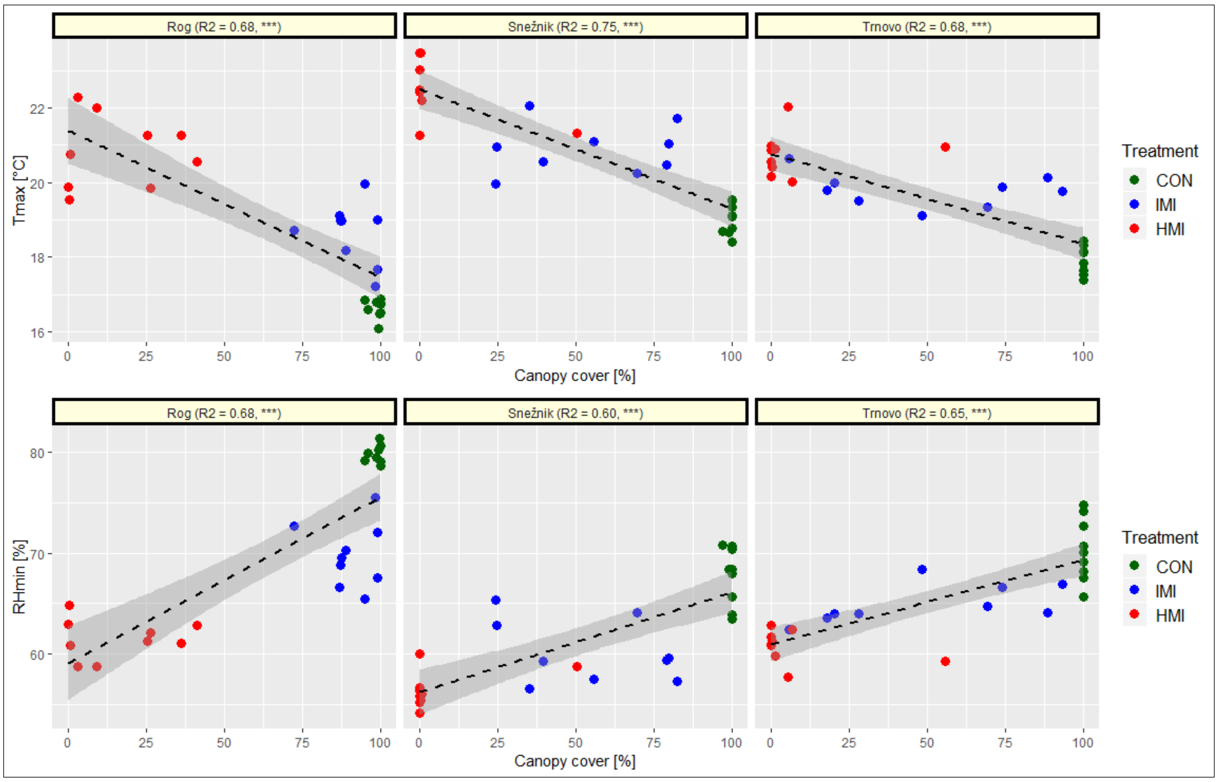

Figure 5: Linear relationship between overstory canopy cover (%, data derived from LiDAR) and daily maximum temperature (T_{max}, upper panels) for different cutting intensities (CON = control, IMI = 50% cut, HMI = 100% cut). Bottom-row panels show linear regressions between canopy cover and daily minimum relative humidity (RH_{min}). Results are reported separately for each study site (Kočevski Rog, Snežnik, Trnovo). Significant regression lines and corresponding 95% envelopes are given. *** $p < 0.001$, R^2 – explained variance by the regression model.

3.5. *Microclimate in relation to topographic factors*

We found significant relations between microclimatic variables and the AspSlo index for plots where cutting was performed (IMI and HMI treatments), whereas the dependence of T_{max} and RH_{min} on the AspSlo index in CON plots was not significant (Fig. 6). There was a significant ($p < 0.05$) positive linear relation between the AspSlo index and T_{max} in HMI plots. In IMI plots this regression was marginally significant ($p < 0.1$). The relationship between the AspSlo index and RH_{min} was negative, but only marginally significant in HMI plots. In general, more exposed steep south-facing plots experienced high T_{max} and low RH_{min} values (Fig. 6).

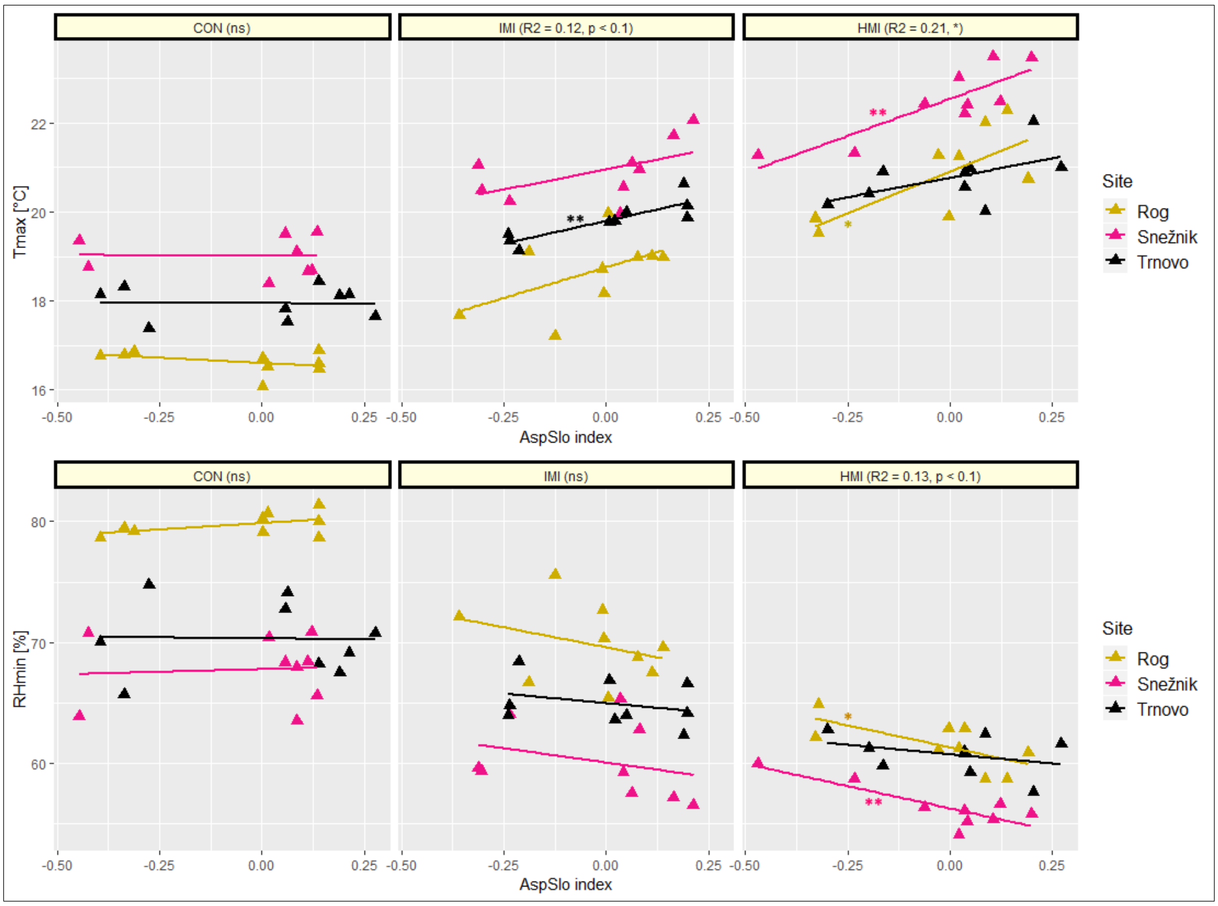

Figure 6: Linear regression between the AspSlo index and maximum daily temperature T_{max} (upper panels) and minimum daily relative humidity RH_{min} (bottom panels). The AspSlo index combines both slope aspect and slope inclination. Regressions are made separately for each cutting treatment (control = CON, 50% cut = IMI, 100% cut = HMI) and study site (Kočevski Rog, Snežnik, Trnovo). Asterisks beside the regression lines indicate that the slope of the regression line is significantly different from zero (** $p < 0.01$, * $p < 0.05$). R^2 – explained variance by the regression model.

4. Discussion

4.1. Response of microclimate to overstory removal at different time scales

Our experimental research in Dinaric fir-beech forests in Slovenia gave us an opportunity to observe differences in microclimate between forest stands subjected to different management intensities, and our results are in agreement with those of numerous studies (e.g. Chen et al., 1993; Heithecker and Halpern, 2006; Kovács et al., 2018). Differences in microclimatic variables between treatments corresponded to the intensity of stand growing stock (canopy cover) removal. Kovács et al. (2018) showed that clear-cuts in oak-hornbeam stands induced extreme light increment and consequently substantially increased air temperature and vapour pressure deficit. In our study, closed-canopy forests also had a cooling effect, expressed as lower T_{max}, and a humidifying effect, expressed as higher RH_{min}, due to the dense canopy cover which intercepted a substantial proportion of solar radiation.

We found that the IMI treatment (50% cut) resulted in significant divergence from the uncut controls in all investigated microclimatic variables. Differences in microclimate were on average lower between the IMI and HMI treatments than between the IMI and CON treatments. Even though the mean and maximum values of microclimatic variables in IMI treatment were consistently lower than those in HMI treatment, the overall observation is that IMI treatment acted slightly more similarly to the HMI treatment than to the CON treatment. These results are in contrast to some previous studies which quantified the effects of partial cutting on forest microclimate. Heithecker and Halpern (2006) reported that T_{avg} and T_{max} did not differ significantly between a treatment with 40% dispersed retention of stand basal area and control. Kovács et al. (2018) illustrated that uniform partial cutting in oak-hornbeam forest, where 30% of the initial total basal area of the upper canopy layer was cut (plus complete sub-canopy and shrub layer removal), significantly differed from uncut stands with respect to T_{avg} only, but not with respect to RH_{avg} and VPD_{avg}. The significant deviation of the IMI treatment from the CON treatment in our case is most likely because of more intensive cutting compared to other similar studies (e.g. Heithecker and Halpern, 2006; Kovács et al., 2018).

High management intensity was characterized by the highest T and VPD, as well as the lowest RH values. Daily T_{avg} in HMI plots was on average ca. 1 °C higher compared to CON plots.

This is in line with previous studies of Carlson and Groot (1997), von Arx et al. (2013) and Kovács et al. (2018). However, mean differences in daily T_{max} and VPD_{max} (CON vs. HMI: 3.5 °C and 0.6 kPa, respectively) were significantly higher and also consistent with those reported in other studies (e.g. mean buffering capacity for T: 1.5 °C to 5 °C) spanning different forest types (Morecroft et al., 1998; von Arx et al., 2013; Davis et al., 2019). For instance, von Arx et al. (2013) showed that the long-term mean buffering capacity of 11 different temperate forest types was up to 3.3 °C for daily T_{max} and 0.52 kPa for daily VPD_{max}. Renaud et al. (2010) highlighted that in beech and beech-silver fir forests, T_{max} during summer was 6 to 8 °C lower below-canopy compared to open-field, and RH_{min} was most often 10% to 20% higher in forest than in the open-field. A recent study of understory temperature buffering in temperate deciduous forests across Europe (Zellweger et al., 2019) demonstrated that the maximum temperature during the summer was on average cooler by 2.1 °C inside than outside forests. Moreover, a global analysis of understory versus open temperature offset showed that the mean and maximum understory temperatures were, on average, cooler by 1.7 °C and 4.1 °C, respectively. Conversely, the minimum temperatures were 1.1 °C warmer under forest canopies than outside the forest (De Frenne et al., 2019).

Our field data were analysed for the buffering capacity of the canopy with respect to seasonal and diurnal patterns. The prevailing seasonal pattern revealed that (1) differences between treatments were highest during the summer months and (2) largely depended on the general weather conditions. A greater buffering effect of forest canopy in summer, particularly when considering T_{max}, has also been reported by Morecroft et al. (1998), von Arx et al. (2012) and Baker et al. (2014). Summer is a period of maximum leaf canopy development when the presence of foliage enhances the difference between closed forests and canopy gaps. During clear, hot and dry summer days, when conditions are physiologically most demanding for plant growth, differences in T_{max} between the CON and the HMI treatments were on average significantly higher (~ 5 °C) than during more cloudy, cold and wet days in autumn (~ 1 °C). There is also a significant inter-seasonal variation in the buffering capacity of intact forest canopies. Thom et al. (2020) showed higher microclimatic buffering capacity of undisturbed European beech forest in warm and dry years due to increase in evaporation causing additional cooling and wetting of the air. Our results and those of other studies confirm that the temperature offset is magnified as temperatures become more extreme (De Frenne et al., 2019).

Clear differences in the diurnal cycles of T and RH were found between silvicultural measures. Buffering capacity below dense canopy (CON treatment) was strongest in early afternoon when maximum temperatures in HMI plots evidently exceeded those in the other two treatment types. In addition, we showed that the microclimate in the forest interior would track open area (canopy gap) conditions with some time lag. This is contrary to von Arx et al. (2013), who showed that the timing of T_{min}, T_{max}, RH_{min} and RH_{max} in forest stands and nearby open areas more or less coincided, i.e. time lags were generally less than 30 min. Such time lags were also not confirmed in the study by Holst et al. (2004) in a Central European beech forest and by Morecroft et al. (1998) in an oak woodland.

4.2. Canopy cover and local topography as drivers of microclimate at a fine spatial scale

We found that forest stand structure factors played an important role in driving evident differences in microclimate between stands subjected to different management intensities. Microclimate buffering was most strongly related to canopy cover, which is consistent with other studies (von Arx et al., 2013; Hardwick et al., 2015; Kovács et al., 2017; Greiser et al., 2018). Davis et al. (2019) found that canopy buffering of T and VPD was greater at higher levels of canopy cover. Zellweger et al. (2019) concluded that local canopy cover was a strong non-linear driver of the maximum temperature offset during summer. Furthermore, topographic factors (slope exposition and steepness) contributed to spatial variability in microclimate, which is in line with many previous studies (e.g. Grimmond et al., 2000; Ma et al., 2010; Macek et al., 2019). Jucker et al. (2018) found that canopy structure and topography jointly constrain the local microclimate of human-modified tropical landscapes.

Our results pointed to the significant dependence of T_{max} and RH_{min} on the degree of canopy closure, suggesting its clear dampening effect on microclimate extremes. The air temperature in plots with higher canopy cover was lower and the air was more humid. Canopy cover is a major determinant of the amount of solar radiation reaching the forest floor (Morecroft et al., 1998). Previous studies demonstrated that, in general, the buffering capacity of the forests is mainly related to factors associated with overstory structure, e.g. leaf area index or canopy cover, tree height and structural heterogeneity (Renaud et al., 2010; Hardwick et al., 2015; Ehbrecht et al., 2019). Ehbrecht et al. (2019) concluded that structural characteristics of forest stands other than canopy openness marginally contribute to variation in forest microclimate. The results of Kovács et al. (2017) suggested that structural elements have a stronger influence on microclimate conditions than the tree species composition of the overstory layer.

The effects of cutting treatments were, at least to some degree, modified due to the specific topographic features of karst sinkholes. Within-sinkhole position had a significant impact on microclimatic conditions. The more exposed south-facing plots in the HMI treatment experienced the most extreme microclimatic conditions (i.e. highest T and lowest RH overall). Slope aspect is also important within forests with closed canopy, as shown by Grimmond et al. (2000). However, position within the sinkhole did not significantly affect microclimate in our control stands. In contrast, the spatial variability of microclimate increased along the cutting intensity gradient, meaning that differences between within-sinkhole positions were more pronounced in treated stands. All of these results suggest that overstory removal increased the dependence of microclimate on local topographic factors.

In general, south-facing and north-facing plots differed the most for the majority of meteorological variables. However, for T_{max} (Fig. 2b), the largest differences were between central and north-facing plots. This could be explained either by cold air accumulation in the centre of the sinkholes or by slight differences in the slope and shape (DDratio) of the sinkholes between treatment types (Table S1 in the Supplementary material). The observed pattern could also be attributed to environmental factors (e.g. soil properties, ground vegetation cover, bare soil cover) which were not measured in our study but described in other studies (e.g. Sewerniak and Puchałka, 2020).

4.3. Ecological relevance of the observed microclimatic patterns for forest vegetation and management implications

Our results and other empirical evidence (Heithecker and Halpern, 2007; Abd Latif and Blackburn, 2010; Ma et al., 2010; Hardwick et al., 2015; Kovács et al. 2018; Thom et al., 2020) highlight how management and natural forest disturbances drive changes in microclimate. The highest value for each microclimatic variable was more likely to occur in disturbed stands, indicating that cutting can induce more extreme microclimatic conditions. Based on experimental (e.g. Lendzion and Leuschner, 2008; Will et al., 2013) and observational studies (e.g. Leuschner and Lendzion, 2009; Park Williams et al. 2013), we can assume that the magnitude of the described differences in microclimate between treatments has an eco-physiologically meaningful effect on forest-dwelling organisms and a marked impact on many bioecological processes. Macek et al. (2019) demonstrated that maximum air temperature, which is controlled by landscape topography, affects plant species composition in temperate forests. Topographically induced variation in microclimate and soil conditions similarly drive ground vegetation diversity in secondary forest ecosystems, such as managed *Pinus sylvestris* mono-stands on inland dunes (Sewerniak and Puchałka, 2020).

An increase in temperature and especially VPD directly affect plant survival, growth and reproduction (Davis et al., 2019). If extreme microclimatic conditions, such as higher temperatures in the daytime (or summer months) and cooler ones in the night-time (or winter months), exceed tolerance thresholds for certain species, growth patterns and species composition will likely be altered (Ma et al., 2010; Jucker et al., 2018; Buras and Menzel, 2019). High T_{max} and VPD_{max} during the warmest and driest time of the day, coupled with high short-term fluctuations and diurnal variation in microclimatic conditions can cause stress for plants, potentially resulting in regeneration failure of the currently prevailing tree species (Thom et al., 2020). There seems to be a critical threshold canopy density below which the buffering capacity of forest ecosystems switches from supportive (buffering capacity of forest canopy strongest when conditions most demanding) to unsupportive (buffering capacity on microclimate small to negative when conditions most demanding) (von Arx et al., 2013) for tree species regeneration and growth of forest-dependent herbaceous understory plant communities (De Frenne et al., 2013). Stressful microclimatic conditions can act as a strong filtering force, especially for shade-tolerant, late-successional plant species with low drought tolerance, which are adapted to a more stable and less stressful microclimate, and thus induce significant control over early succession pathways in post-cutting forest stands (Taylor et al., 2020).

Under karstic conditions with a high number of sinkholes, forest management practices must be adapted to very rough and sensitive terrain (Kobal et al., 2015; Aguilon et al., 2020). Forest managers and silviculturalists could benefit from our findings. For example, when planning artificial tree regeneration to restore damaged or open forest areas, the planting of sensitive climax tree species (such as *Abies alba*) should be avoided in microsites within canopy gaps (HMI treatment) with the highest heat load and most extreme microclimate (steep south-facing slopes), as indicated by high VPD. Young trees are most strongly affected by microclimate-induced stress, as their root systems do not yet reach deep into the soil (Thom et al., 2020). Even partial reduction of the canopy cover (IMI treatment) induced significant differences in microclimate compared to the CON treatment. Lower levels of canopy removal should be implemented on south-facing slopes to mitigate the effects on ground microclimate. In contrast, north-facing slopes receive less insolation than surrounding areas and usually have more favourable microclimatic conditions (lower T and higher RH) for typical forest plant species with affinity to shadier microsites. Such effects can facilitate *in situ* persistence of pre-disturbance compositional legacy, positive response of shade-tolerant trees and general co-existence of ecological divergent plant species in post-treatment conditions. Greater focus on these relationships may contribute not only to more effective forest management, but also to reduced loss of soil organic matter and maintenance of high diversity of plant communities (Jasińska et al., 2020; Sewerniak and Puchałka, 2020; Kiss et al., 2020).

We emphasize the importance of canopy cover for the buffering capacity of forest microclimate. The provision of this basic stand structural feature is expected to be seriously at risk as forest disturbances around the globe are likely to have a strong impact on canopy structure in the future (Lenoir et al., 2017). Variety of anthropogenic disturbances alter the conservation value of karst dolines (Bátori et al., 2020). Kiss et al. (2020) concluded that intensive logging, the main driver of changes in forest cover, decrease the capacity of depressions to support beech and ravine forest species. The buffering capacity of temperate forests might decrease due to the increasing impacts of more frequent and intense disturbances as well as extreme weather events resulting in drought- and heat-stress (Park Williams et al., 2013; Thom et al., 2017; Davis et al., 2019). High disturbance severity paired with a large disturbance extent will have particularly strong impacts on forest microclimate (Baker et al., 2014; Davis et al., 2019). Practitioners should in general intensify their efforts to foster the microclimatic buffering capacity of forest canopies to mitigate hot and dry weather conditions. Strategies to improve the microclimate need to be adapted locally considering the specific stand and site conditions (Thom et al., 2020). Moreover, due to the combination of specific site conditions and unfavourable factors, such as reduced mechanical and biological stability of forest stands as a consequence of intense large-scale disturbances, prolonged summer droughts, water-permeable karst terrain and associated shallow soils with low water storage capacity, Dinaric fir-beech forests are presumed to be highly susceptible to global climate change (Kutnar and Kobler, 2011).

4.4. Conclusions

The short-term responses of microclimatic conditions in Dinaric fir-beech forests to various forest management intensities showed that the greatest differences were observed between the most intensive treatment and the uncut controls. Obtained results corroborate the widespread microclimatic patterns recognized in forested areas with highly diversified land terrain, spanning from lowland to mountain regions. The effects of overstory removal might interact with local topographic factors, as shown by our results, where spatio-temporal variations in temperature and relative humidity were jointly driven by canopy cover and terrain topography (slope aspect and slope inclination). Overstory removal increased the dependence of microclimate upon local topographic factors. In general, the results highlight the intricate interplay between many environmental factors in forest ecosystems which might significantly affect understory species occurrence, tree seedling growth and thereby overall forest structure and composition. The main findings of our research should be considered in forest management planning and forest biodiversity protection.

Acknowledgements

The research was partially funded by the European LIFE ManFor C.BD Project (LIFE09 ENV/IT/000078) and the Slovenian Research Agency core funding for the Programme Groups P4-0107 and P4-0085. Janez Kermavnar received funding from the Slovenian Research Agency as part of the Young Researcher Programme (Contract no. 1000-18-0404). We would like to express our gratitude to colleagues from the Slovenian Forestry Institute for their assistance in various areas and many experts from the Slovenian Forest Service for their help with the field preparation during this experimental study. We thank the anonymous reviewers for their many constructive comments on an earlier version of the manuscript. We are grateful to Philip J. Nagel for language correction.

The authors of this manuscript have no conflict of interest to declare.

5. References

Abd Latif, Z., Blackburn, G.A., 2010. The effects of gap size on some microclimate variables during late summer and autumn in a temperate broadleaved deciduous forest. Int. J. Biometeorol. 54, 119-129.

Aguilon, D.J., Vojtkó, A., Tölgyesi, C., Erdős, L., Kiss, P.J., Lőrinczi, G., Juhász, O., Frei, K., Bátori, Z., 2020. Karst environments and disturbance: evaluation of the effects of human activity on grassland and forest naturalness in dolines. Biologia, https://doi.org/10.2478/s11756-020-00518-7

Ashcroft, M.B., Gollan, J.R. 2013. Moisture, thermal inertia, and the spatial distributions on near-surface soil and air temperatures: Understanding factors that promote microrefugia. Agric. For. Meteorol. 176, 77-89.

Aussenac, G., 2000. Interactions between forest stands and microclimate: Ecophysiological aspects and consequences for silviculture. Ann. For. Sci. 57 (3), 287-301.

Baker, T.P., Jordan, G.J., Steel, E.A., Fountain-Jones, N.M., Wardlaw, T.J., Baker, S.C., 2014. Microclimate through space and time: Microclimatic variation at the edge of regeneration forests over daily, yearly and decadal time scales. Forest Ecol. Manag. 334, 174-184.

Bátori, Z., Vojtkó, A., Keppel, G., Tölgyesi, C., Čarni, A., Zorn, M., Farkas, T., Erdős, L., Kiss, P.J., Módra, G., Breg Valjavec, M., 2020. Anthropogenic disturbances alter the conservation value of karst dolines. Biodiversity and Conservation 29: 503-525.

Bartoń, K., 2019. MuMIn: Multi-Model Inference, R Package Version 1.43.6. Available online: https://cran.r-project.org/web/packages/MuMIn/MuMIn.pdf

Buras, A., Menzel, A., 2019. Projecting Tree Species Composition Changes of European Forests for 2061-2090 Under RCP 4.5 and RCP 8.5 Scenarios. Front. Plant Sci. 9, 1986.

Cantlon, J.E., 1953. Vegetation and microclimates on north and south slopes of Cushetunk Mountain, New Jersey. Ecol. Monogr. 23, 241-270.

Carlson, D.W., Groot, A., 1997. Microclimate of clear-cut, forest interior, and small openings in trembling aspen forest. Agric. For. Meteorol. 87, 313-329.

Chen, J., Franklin J.F., Spies, T.A., 1993. Contrasting microclimates among clearcut, edge, and interior of old-growth Douglas-fir forest. Agric. For. Meteorol. 63, 219-237.

Davis, K.T., Dobrowski, S.Z., Holden, Z.A., Higuera, P.E., Abatzoglou, J.T., 2019. Microclimatic buffering in forests of the future: the role of local water balance. Ecography 42, 1-11.

De Frenne, P., Rodríguez-Sánchez, F., Coomes, D.A., Baeten, L., Verstraeten, G., Vellend, M., Bernhardt-Römermann, Brown, C.D., Brunet, J., Cornelis, J., Decocq, G.M., Dierschke, H., Eriksson, O., Gilliam, F.S., Hédl, R., Heinken, T., Hermy, M., Hommel, P., Jenkins, M.A., Kelly, D.L., Kirby, K.J., Mitchell, F.J.G., Naaf, T., Newman, M., Peterken, G., Petřík, P., Schultz, J., Sonnier, G., Van Calster, H., Waller, D.M., Walther, G.-R., White, P.S., Woods, K.D., Wulf., M., Graae, B.J., Verheyen, K., 2013. Microclimate moderates plant responses to macroclimate warming. PNAS 110 (46), 18561-18565.

De Frenne, P., Zellweger, F., Rodríguez-Sánchez, F., Scheffers, B.R., Hylander, K., Luoto, M., Vellend, M., Verheyen, K., Lenoir J., 2019. Global buffering of temperatures under forest canopies. Nat. Ecol. Evol. 3, 744-749.

Ehbrecht, M., Schall, P., Ammer, C., Fischer, M., Seidel, D., 2019. Effects of structural heterogeneity on the diurnal temperature range in temperate forest ecosystems. Forest Ecol. Manag. 432, 860-867.

Faraway, J.J., 2006. Extending the Linear Model with R: Generalized Linear, Mixed Effects and Nonparametric Regression models. Chapman and Hall/CRC: Boca Raton, FL, USA.

Fleming, R.L., Baldwin, K.A., 2008. Effects of harvest intensity and aspect on a boreal transition tolerant hardwood forest. I. Initial postharvest understory composition. Can. J. Forest Res. 38 (4), 685-697.

Forest Act, 1993. The Law on Forests (Official Gazette of RS, Nos. 30/93 , 56/99 - ZON, 67/02 , 110/02 - ZGO-1 115/06 - ORZG40, 110/07 , 106/10 , 63/13 , 101/13 - ZDavNepr, 17/14 , 22/14 - dec. US, 24/15 , 9/16 - ZGGLRS and 77/16. Available online: http://pisrs.si/Pis.web/pregledPredpisa?id=ZAKO270 (accessed 13 August 2019).

Frey, S.J.K., Hadley, A.S., Johnson, S.L., Schulze, M., Jones, J.A., Betts, M.G., 2016. Spatial models reveal the microclimatic buffering capacity of old-growth forests. Sci. Adv. 2 (4), e1501392.

Greiser, C., Meineri, E., Luoto, M., Ehrlén, J., Hylander, K., 2018. Monthly microclimate models in a managed boreal forest landscape. Agric. For. Meteorol. 250-251, 147-158.

Grimmond, C.S.B., Robeson, S.M., Schoof, J.T., 2000. Spatial variability of micro-climatic conditions within a mid-latitude deciduous forest. Clim. Res. 15, 137-149.

Hardwick, S.R., Toumi, R., Pfeifer, M., Turner, C.E., Nilus, R., Ewers, R.M., 2015. The relationship between leaf area index and microclimate in tropical forest and oil palm plantation: Forest disturbance drives changes in microclimate. Agric. For. Meteorol. 201, 187-195.

Heithecker, T.D., Halpern, C.B., 2006. Variation in microclimate associated with dispersed-retention harvests in coniferous forests of western Washington. Forest Ecol. Manag. 226, 60-71.

Heithecker, T.D., Halpern, C.B., 2007. Edge-related gradients in microclimate in forest aggregates following structural retention harvest in western Washington. Forest Ecol. Manag. 248, 163-173.

Holst, T., Mayer, H., Schindler, D., 2004. Microclimate within beech stands-part II: thermal conditions. Eur. J. Forest. Res. 123, 13-28.

Hothorn, T., Bretz, F., Westfall, P., 2019. Multcomp: Simultaneous Inference in General Parametric Models, R Package Version 1.40-10. Available online: https://cran.r-project.org/web/packages/multcomp/multcomp.pdf (accessed 15 June 2019).

Hyndman, R., Athanasopoulos, G., Bergmeir, C., Caceres, G., Chhay, L., O'Hara-Wild, Petropoulos, F., Razbash, S., Wang, E., Yasmeem, F., 2019. forecast: Forecasting functions for time series and linear models, R Package version 8.9. Available online: https://cran.r-project.org/web/packages/forecast/forecast.pdf (accessed 22 January 2019).

IUSS Working Group WRB, 2015. World reference base for soil resources 2014, updated 2015. International soil classification system for naming soils and creating legends for soil maps. World Soil Resources Reports No. 106, 192 p., Rome, Italy: FAO.

Jasińska, J., Sewerniak, P., Puchałka, R., 2020. Litterfall in a Scots Pine Forest on Inland Dunes in Central Europe: Mass, Seasonal Dynamics and Chemistry. Forests 11, 678.

Jucker, T., Hardwick, S.R., Both, S., Elias, D.M.O., Ewers, R.M., Milodowski, D.T., Swinfield, T., Coomes, D.A., 2018. Canopy structure and topography jointly constrain the microclimate of human-modified tropical landscapes. Glob. Change Biol. 24, 5243-5258.

Keenan, R.J., Kimmins, J.P., 1993. The ecological effects of clear-cutting. Environ. Rev. 1 (2), 121-144.

Kiss, P.J., Tölgyesi, C., Bóni, I., Erdős, L., Vojtkó, A., Maák, I.E., Bátori, Z., 2020. The effects of intensive logging on the capacity of karst dolines to provide potential microrefugia for cool-adapted plants. Acta Geogr. Slov. 60-1, 37-48.

Kobal, M., Bertoncelj, I., Pirotti, F., Dakskobler, I., Kutnar, L., 2015. Using Lidar Data to Analyse Sinkhole Characteristics Relevant for Understory Vegetation under Forest Cover – Case Study of a High Karst Area in the Dinaric Mountains. PLoS ONE 10(3): e0122070.

Kovács, B., Tinya, F., Ódor, P., 2017. Stand structural drivers of microclimate in mature temperate mixed forests. Agric. For. Meteorol. 234-235, 11-21.

Kovács, B., Tinya, F., Guba, E., Németh, C., Sass, V., Bidló, A., Ódor, P., 2018. The Short-Term Effects of Experimental Forestry Treatments on Site Condition in an Oak-Hornbeam Forest. Forests 9, 406.

Kutnar, L., Kobler, A., 2011. Prediction of forest vegetation shift due to different climate-change scenarios in Slovenia. Sumar List. 135, 113-126.

Kutnar, L., Eler, K., Marinšek, A., 2015. Effects of different silvicultural measures on plant diversity – the case of the Illyrian *Fagus sylvatica* habitat type (Natura 2000). iForest 9, 318-324.

Lendzion, J., Leuschner, C., 2008. Growth of European beech (*Fagus sylvatica* L.) saplings is limited by elevated atmospheric vapour pressure deficits. For. Ecol. Manag. 256, 648-655.

Lenoir, J., Hattab, T., Pierre, G., 2017. Climatic microrefugia under anthropogenic climate change: implications for species redistribution. Ecography 40, 253-266.

Lenth, R.V., 2016. Least-Squares Means: The R Package lsmeans. J. Stat. Soft. 69.

Leuschner, C. Lendzion, J., 2009. Air humidity, soil moisture and soil chemistry as determinants of the herb layer composition in European beech forests. J. Veg. Sci. 20, 288-298.

Ma, S., Concilio, A., Oakley, B., North, M., Chen, J., 2010. Spatial variability in microclimate in a mixed-conifer forest before and after thinning and burning treatments. Forest Ecol. Manag. 259, 904-915.

Macek, M., Kopecký, M., Wild, J., 2019. Maximum air temperature controlled by landscape topography affects plant species composition in temperate forests. Landscape Ecol. 34, 2541-2556.

Morecroft, M.D., Taylor, M.E., Oliver, H.R., 1998. Air and soil microclimates of deciduous woodland compared to an open site. Agric. For. Meteorol. 90, 141-156.

Murray, F.W., 1967. On the computation of the saturation vapor pressure. J. Appl. Meteorol. 6, 203-204.

Nagel, T.A., Mikac, S., Dolinar, M., Klopčič, M., Keren, S., Svoboda, M., Diaci, J., Bončina, A., Paulić, V., 2017. The natural disturbance regime in forests of the Dinaric Mountains: A synthesis of evidence. For. Ecol. Manag. 388, 29-42.

Park Williams, A., Allen, C.D., Macalady, A.K., Griffin, D., Woodhouse, C.A., Meko, D.M., Swetnam, T.W., Rauscher, S.A., Seager, R., Grissino-Mayer, H.D., Dean, J.S., Cook, E.R., Gangodagamage, C., Cai, M., McDowell, N.G., 2013. Temperature as a potent driver of regional forest drought stress and tree mortality. Nat. Clim. Change 3, 292-297.

Pinheiro, J., Bates, D., DebRoy, S., Sarkar, D., R Core Team, 2019. nlme: Linear and Nonlinear Mixed Effects Models. R Package Version 3.1-141. Available online: https://cran.r-project.org/web/packages/nlme/nlme.pdf (accessed 23 July 2019).

R Core Team, 2018. R: A language and environment for statistical computing. R Foundation for Statistical Computing. 2018, Vienna, Austria. URL https://www.R-project.org/.

Renaud, V., Innes, J.L., Dobbertin, M., Rebetez, M., 2010. Comparison between open-site and below-canopy climatic conditions in Switzerland for different types of forests over 10 years (1998-2007). Theor. Appl. Climatol. 105 (1-2), 119-127.

Sewerniak, P., Jankowski, M., Dąbrowski, M., 2017. Effect of topography and deforestation on regular variation of soils on inland dunes in the Toruń Basin (N Poland). Catena 149, 318-330.

Sewerniak, P., Puchałka, R., 2020. Topographically induced variation of microclimatic and soil conditions drives ground vegetation diversity in managed Scots pine stands on inland dunes. Agric. For. Meteorol. 291, 108054.

Slovenian Environment Agency archive, 2019. Archive of measurements – observed and measured meteorological data in Slovenia. http://meteo.arso.gov.si/met/sl/archive/ (accessed November 2018).

Suggitt, A.J., Gillingham, P.K., Hill, J.K., Huntley, B., Kunin, W.E., Roy, D.B., Thomas, C.D., 2011. Habitat microclimates drive fine-scale variation in extreme temperatures. Oikos 120, 1-8.

Taylor, A.R., Endicott, S., Hennigar, C., 2020. Disentangling mechanisms of early succession following harvest: Implications for climate change adaptation in Canada's boreal-temperate forests. Forest Ecol. Manag. 461, 117926.

Thom, D., Rammer, W., Seidl, R., 2017. The impact of future forest dynamics on climate: interactive effects of changing vegetation and disturbance regimes. Ecol. Monogr. 87 (4), 665-684.

Thom, D., Sommerfeld, A., Sebald, J., Hagge, J., Müller, J., Seidl, R., 2020. Effects of disturbance patterns and deadwood on the microclimate in European beech forests. Agric. For. Meteorol. 291, 108066.

von Arx, G., Dobbertin, M., Rebetez, M., 2012. Spatio-temporal effects of forest canopy on understory microclimate in a long-term experiment in Switzerland. Agric. For. Meteorol. 166-167, 144-155.

von Arx, G., Graf Pannatier, E., Thimonier, A., Rebetez, M., 2013. Microclimate in forests with varying leaf area index and soil moisture: potential implications for seedling establishment in a changing climate. J. Ecol. 101, 1201-1213.

Will, R.E., Wilson, S.M., Zou, C.B., Hennessey, T.C., 2013. Increased vapor pressure deficit due to higher temperature leads to greater transpiration and faster mortality during drought for tree seedlings common to the forest-grassland ecotone. New. Phytol. 200, 366-374.

Zellweger, F., Coomes, D., Lenoir, J., Depauw, L., Maes, S., Wulf, M., Kirby, K.J., Brunet, J., Kopecký, M., Máliš, F., Schmidt, W., Heinrichs, S., den Ouden, J., Jaroszewicz, B., Buyse, G., Spicher, F., Verheyen, K., De Frenne, P., 2019. Seasonal drivers of understory temperature buffering in temperate deciduous forests across Europe. Global Ecol. Biogeogr. 28, 1774-1786.

Zheng, D., Chen, J., Song, B., Xu, M., Sneed, P., Jensen, R., 2000. Effects of silvicultural treatments on summer forest microclimate in southeastern Missouri Ozarks. Clim. Res. 15, 45-59.

Zuur, A.F., Ieno, E.N., Walker, N.J., Saveliev, A.A., Smith, G.M., 2009. Mixed effect models and extensions in ecology with R. 574 p., New York, NY: Springer.

Supplementary material, Table S1:

Selected geomorphological parameters (calculated based on LiDAR data for north-south and east-west transects) of karst sinkholes, averaged across three study sites for each treatment type (CON = control, IMI = 50 % cut, HMI = 100 % cut): elevation (m), depth of the sinkhole (m, i.e. elevation difference between the bottom and edge of the sinkhole), radius (distance between the centre and edge of the sinkhole), slope (%) and DDratio (diameter vs. depth ratio). The latter describes the ratio between the diameter (radius × 2) and depth of the sinkhole. It gives a very rough estimation of the shape of the sinkhole. The higher the DDratio, the more "open" the sinkhole is. Sinkholes with a lower DDratio are more "closed", i.e. their depth is relatively large compared to their diameter. Potential differences between treatments were tested with a non-parametric Kruskal-Wallis Rank sum test (alpha = 0.05).

The values are mean ± SD. n.s. – non-significant differences between treatments.

TREATMENT	Elevation (m)	Depth (m)	Radius (m)	Slope (%)	DDratio
CON	803.8 ± 42.7	9.8 ± 3.0	32.7 ± 10.9	32.6 ± 4.0	6.7 ± 1.0
IMI	788.0 ± 42.4	9.3 ± 2.2	32.8 ± 7.8	30.6 ± 3.5	7.1 ± 1.1
HMI	789.7 ± 48.1	7.9 ± 3.3	29.9 ± 9.6	26.6 ± 6.9	8.1 ± 2.0
Kruskal-Wallis test	n.s.	n.s.	n.s.	n.s.	n.s.

Supplementary material, Figure S1:

Daily differences (mean ± SD) in maximum temperature (T_{max}, upper left), diurnal temperature range (DTR, upper right), minimum relative humidity (RH_{min}, bottom left) and maximum vapour pressure deficit (VPD_{max}, bottom right) between cutting treatments: CON vs. HMI, CON vs. IMI and IMI vs. HMI (CON = control, IMI = 50% cut, HMI = 100% cut). Colours denote two different periods: black – summer (JJA) = summer months (June, July and August), grey – transition period (MSO) = May, September and October. Daily differences were averaged across the entire measurement period (three growing seasons), three study sites and within-sinkhole positions (i.e. central, south-facing, north-facing plots).